Progress In Electromagnetics Research M, Vol. 17, 29–42, 2011

COPLANAR MEMS PHASED ARRAY ANTENNA USING KOCH FRACTAL GEOMETRY

M. Jahanbakht

Shahr e Qods Branch
Islamic Azad University, Iran

A. A. Lotfi Neyestanak

Shahr_e_Rey Branch
Islamic Azad University, Tehran, Iran

Abstract—A 3-bit phase array system including phase shifter blocks and antenna elements has been developed on a coplanar waveguide (CPW) using micro electromechanical system (MEMS) technology. The non Euclidean Koch fractal geometry has been used to improve the frequency behavior of the entire system. It is shown that the fractal geometry makes the design to have lower profile, wider frequency bandwidth, and lower mutual coupling effects. It also decreases the actuation voltage of the MEMS switch elements. The fabrication process has been fully described and the measured values regarding every single block is presented.

1. INTRODUCTION

Miniature phased array antennas are employed in many branches of science and technology including automotive radar sensors, mobile applications, and biomedical for their flexibility and beam forming characteristics.

In [1], design considerations are presented for a typical automotive radar application using phased-array antennas based on phase shifters. The phase shifters and SPMT switching networks are presented. They also evaluate two different packaging techniques using glass-frit sealing and polymer sealing. The actuation method used in this reference

Received 3 January 2011, Accepted 10 February 2011, Scheduled 12 February 2011
Corresponding author: Abbas Ali Lotfi Neyestanak (alotfi@iust.ac.ir).

is thermostatic and the entire phased array aspects are not clearly evaluated like antennas or lenses.

Reference [2] describes a one dimensional RF-MEMS phased array for operation at 9.5 GHz. Each antenna is a $4 * 8$ array of patch elements and the phase shifting property is achieved by four 3 bit RF-MEMS phase shifters. The paper explains the hybrid integration of the different blocks in a phased array antenna. The RF-MEMS switch elements used in this phased array are not developed and the actuation voltage is also high.

An integrated 60 GHz CMOS/PCB single-chip digital phased array antenna is presented in [3]. This represents a multi gigabit radio at a similar cost structure as a Bluetooth radio. Furthermore, uncompressed HDMI video streaming is demonstrated in this paper using a standard battery (AAA) operated module. This phased array actually implements semiconductor devices which consume and loss a lot of power compared to RF-MEMS technology.

A stair-planar phased array antenna system is introduced in [4] for mobile broadcast satellite reception in Ku-band. The design procedures for low profile microstrip sub-array, LNA, phase shifters, and the beam forming algorithm are discussed in this paper. This phased array system scans 2.8° in azimuth and 20° in elevation with 3dB scanning loss. Based on the developed algorithm, neither a prior knowledge of the satellite's direction, nor the phase-voltage characteristic of the phase shifters are required. Despite the fact that the system has 2D electronic scanning capability, the height of each antenna element is 6 cm which occupies a relatively wide space for a mobile applications.

In [5], new capabilities of SKA research in Europe are addressed emphasizing the research and development work done and aims to provide insight into the technologies and technical research on calibration, polarization, and side-lobe control that will unleash the potential of phased arrays for future growth of radio astronomy synthesis arrays. This paper barely describes any special idea on any phased array blocks or systems and is extremely low on new ideas or applicable recommends.

MEMS phase shifter has been developed in [6] using inductors. The design consists of a CPW line capacitively and inductively loaded by the periodic set of inductors and electrostatic force actuated MEMS switches as capacitors. The analysis has then been done using ABCD matrix method which is not a reliable method because the coupling effect between cascaded blocks has not been considered.

A novel tunable microwave filter with tuning range of 13.8 to 18.2 GHz fabricated in [7] using a standard silicon foundry process

based on low resistivity silicon substrate. The filter effect has been realized by integrating two inter digitized comb capacitors with a straight line inductor. The tuning effect has been achieved by varying the capacitance value of the capacitors with a bimorph MEMS actuator. The insertion loss of this work varies from 3.5 to 6 dB which is not suitable for lots of applications.

In the following sections the analysis and design process of a 3-bit phased array antenna system would be described and the fabrication process will also been explained in details. Measurement results regarding every single block of the system like antenna elements and phase shifter blocks are presented.

2. THEORY

Fractals are a part of non Euclidean geometries which obviously influenced many branches of science and engineering and that is because of their unique attributes. Designers and engineers have paid lots of attention to the nature of fractal geometries and it has led to many novel works in the new classes of RF applications.

The fractal Koch curves or islands have compact size, low profile, wide frequency bandwidth, and conformal shape in collation with the other fractal models. The self similarity and space filling property in Koch curves make them treat like an infinite length in a certainly finite area.

In the area of MEMS switches and phase shifters, this special trait would decrease the spring constant and increase the effective area of the MEMS phase shifter beam. So the actuation voltage will decrease.

In the area of fractal antennas, these attributes cause the antenna element to have lower profile and also makes it to operate in multiple frequency bands or increases the operating frequency bandwidth. This property of fractal geometries also decreases the unwanted mutual coupling effects between antenna elements in the final compact phased array.

2.1. Fractal Antenna

The antennas and phase shifters of this paper are all fabricated over a silicon substrate with $\varepsilon_r = 11.9$ and thickness of $h = 550\,\mu\text{m}$ and the coplanar waveguide transmission line is used to transmit and deliver microwave power. So there would be no need for any extra transient elements in between.

The fractal Koch antenna profile is shown in Figure 1. The antenna is feed through a coplanar waveguide with $g/w/g$ =

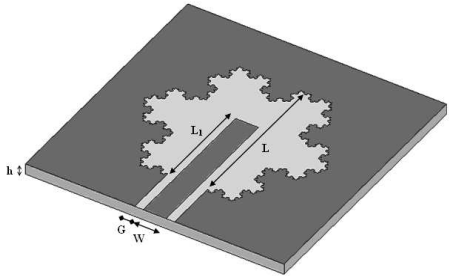

Figure 1. Fractal antenna geometry which is feed by coplanar waveguide.

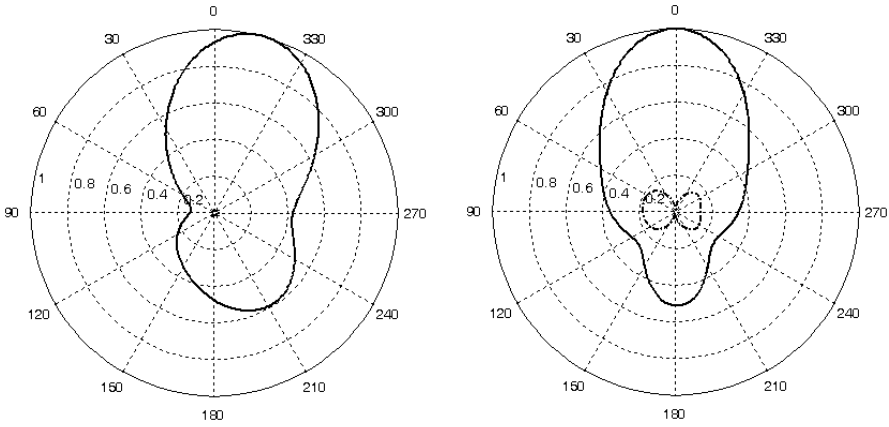

Figure 2. Normalized co (—) and cross (- - -) polarized components of the radiation pattern at 28 GHz.

15/50/15 μm and the number of fractal iterations is choosing to be four [8].

Antenna length is $L = 4$ mm and the tunning stub is fixed on $L_1 = 7{*}L/16$. The smallest part of the antenna has a length of 49.4 μm which makes if proper for small micro-machined hybrid phased array applications.

The operating frequency of the antenna is considered to be 28 GHz. Measured radiation pattern of the antenna element is shown in Figure 2 in both E- and H-planes. As can be seen, the cross polarized component is very small which makes this antenna an appropriate choice for phase array applications.

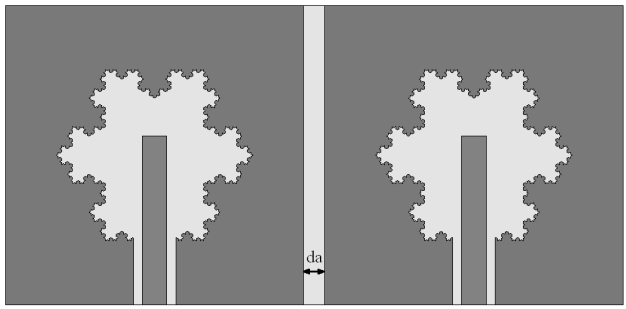

Figure 3. A typical $2 * 1$ array of fractal antennas to evaluate their mutual coupling property.

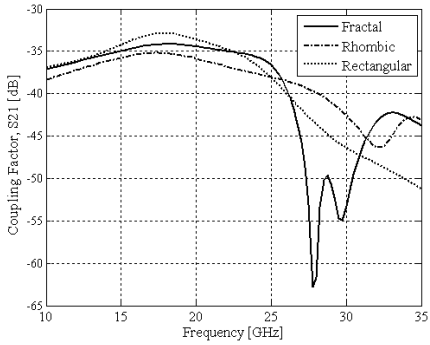

Figure 4. Mutual coupling of a $2 * 1$ array for $da = 5\,\text{mm}$.

One of the major properties of the fractal geometries is their capability to decrease any unwanted mutual coupling effect. Mutual coupling could destroy the desired characteristics of any phased ray system.

In Figure 3, two similar antenna elements are placed in a distance of da from each other to evaluate their mutual coupling effects. The coupling intensity of the antennas in Figure 2 for $da = 5\,\text{mm}$ is shown in Figure 4. The coupling factor of the fractal antenna has been compared with other slot shapes like rhombic and rectangular. As can be seen at the resonant frequency, the mutual coupling of the Koch fractal is almost 15 dB lower than other shapes and geometries.

2.2. Phase Shifter

As can be seen in Figure 5, Koch fractal strip has been used here as curving beam of a MEMS switch. This beam has got the Koch angle

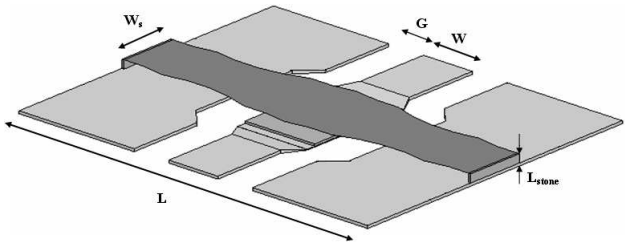

Figure 5. Basis block of the fractal MEMS phase shifter with two Koch iterations.

Table 1. Comparison between the actuation voltages of several MEMS bridges.

Beam Shape	Narrow Rectangle (40 μm)	Wide Rectangle (60 μm)	Elliptical	Fractal	Fractals with more Iterations
Actuation Voltage [v]	25	22	19.5	19	Almost 17

of $\theta = 0.9\pi$ and its length would be choice long enough to cover the entire bridge. The beam length (L) is 250 μm and its width changes from 40 μm to 60 μm at the narrowest and widest positions [9].

The bridge is mounted at 2.5 μm over the central conductor of the bridge and the sputtered silicon nitride isolating layer has height of 0.75 μm preventing bridge from a complete bending. This prevention makes the switch act like a variable capacitor instead of a real on/off switching element [10]. This capacitance causes a change in the wave velocity, creating a small phase shift.

Fractal beam of the Figure 5 is formed by just two stages repetition of the triangular Koch geometry. The effect of the actuation voltage on the deformation of the bridge is investigated in the Figure 6 and compared with other conventional coplanar MEMS phase shifter switches. The required level of this electric potential is extremely depending on the shape of the bridge and its architecture. According to the results of Figure 6 and Table 1, extending the number of fractal iterations got no significant influence on the results and would cause some difficulties on the micromachining process.

The 3-bit phase shifter is developed by cascading 50 number of capacitive switch elements of Figure 5. It is capable of producing any desired phase shifts including 3-bit digital ones named 0, 45, 90, 135, 180, 225, 270, and 315 degrees.

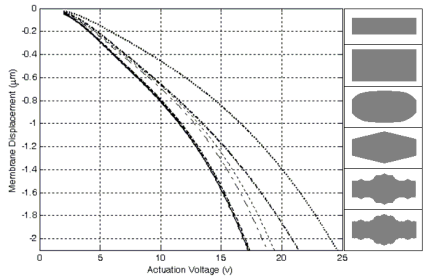

Figure 6. Comparison between the MEMS bridge displacement vs. actuation voltage.

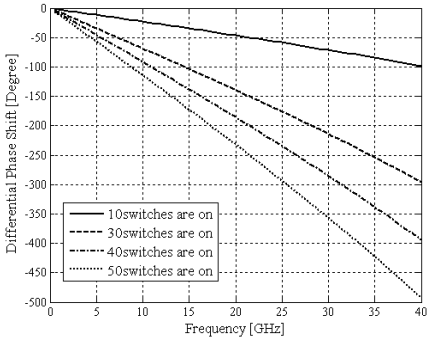

Figure 7. Differential phase shift as a function of frequency for various number of turned on capacitive switches.

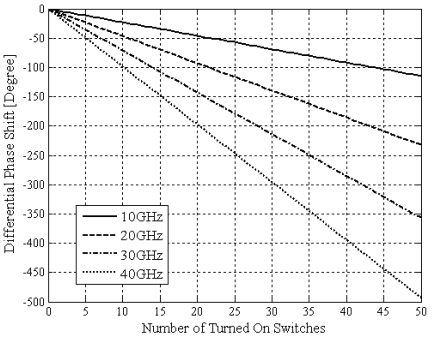

Figure 8. Differential phase shift as a result of turned on capacitive switch numbers for different operating frequencies.

Figures 7 and 8 show the differential phase shift as a function of frequency or the number of turned on switches. As can be seen in these two figures, at the frequency of 28 GHz, any desired phase shift from 0 to 350 degree is achievable.

To produce any desired phase shift at any desired frequency inside the operating frequency range, one ought to combine Figures 7 and 8. The operating frequency of the proposed phased array antenna is chosen to be 28 GHz. According to Figure 7, by turning on all the 50 switches in this frequency, 340 degrees is achievable maximally. This

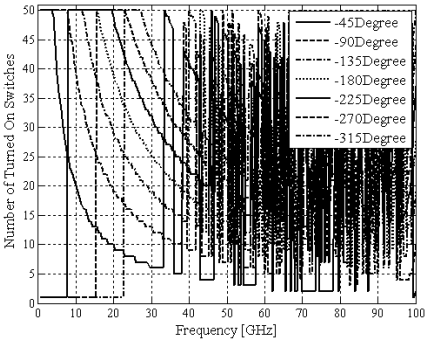

Figure 9. Number of turned on switches as a function of operating frequency to achieve any desired 3-bit phase differences.

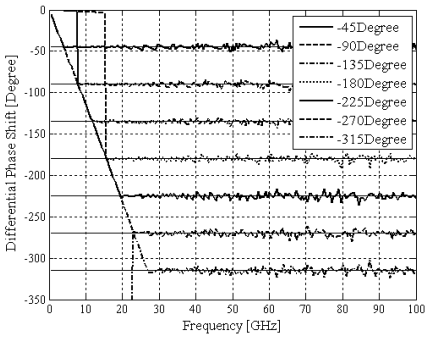

Figure 10. Generating the desired 3-bit phase shifts using a microcontroller block.

is suitable to establish a 3-bit phase shifter with 0, 45, 90, 135, 180, 225, 270, and 315 degrees of phase difference.

This limitation has also been investigated in Figure 8. As can be seen in this figure, the 340° of phase shift is achievable at 28 GHz by turning all the switches on. It worth to mention that by slightly increasing the operating frequency to more than 30 GHz, a 6-bit and more phase shifter could be designed. Combination of Figures 7 and 8 to produce any desired phase difference is done automatically by utilising a microcontroller block and the resulting diagrams are shown in Figures 9 and 10. The microcontroller look up table to turn the switches on or off is presented in Figure 9. This diagram shows how these MEMSs are switched to obtain the values for 3-bit phase shifter. Figure 10 is the result of this operation.

2.3. Phased Array

Using previously described fractal antennas and fractal phase shifters, a $4 * 1$ phased array antenna has been designed and fabricated. To transfer and radiate the maximum power from every antenna element, impedance matching has to be applied.

The impedance matching of array elements is done using optimization tools of the advanced design system (ADS). The ADS block diagram is shown in Figure 11 and the optimization results are presented in Figure 12.

The return loss of the array is less than -40 dB and the feed lines are adjusted to divide power equally between 4 antenna elements by

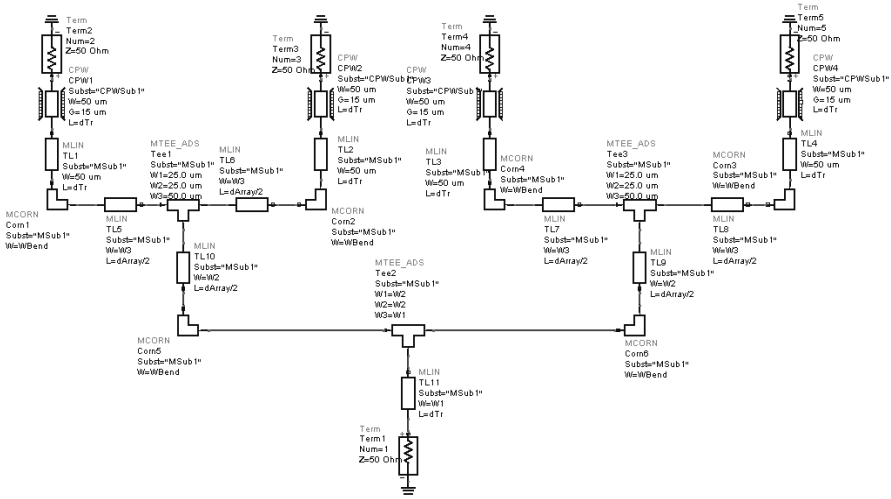

Figure 11. ADS block diagram of a $4 * 1$ phased array antenna used for impedance matching optimization.

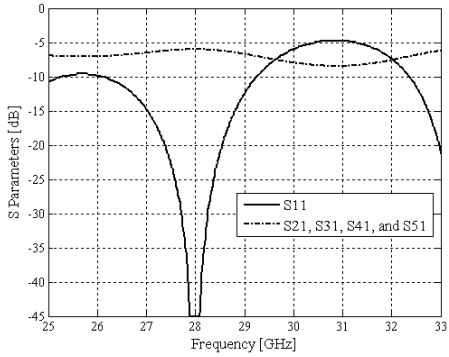

Figure 12. Optimized values of return loss in the $4 * 1$ phased array at 28 GHz.

delivering 1/4 of the total power each. According to the $10 * \log_{10}(x)$, this is equal to -6 dB.

Radiation pattern of the phased array antenna system is plotted in Figure 13. The steering beam property covers more than ± 45 degree in the space above radiating antenna elements.

These radiating fractal antennas are separated by $3\lambda/2$ distance from each other. This beam forming is yielded by the proper operation of the microcontroller block of Figure 10.

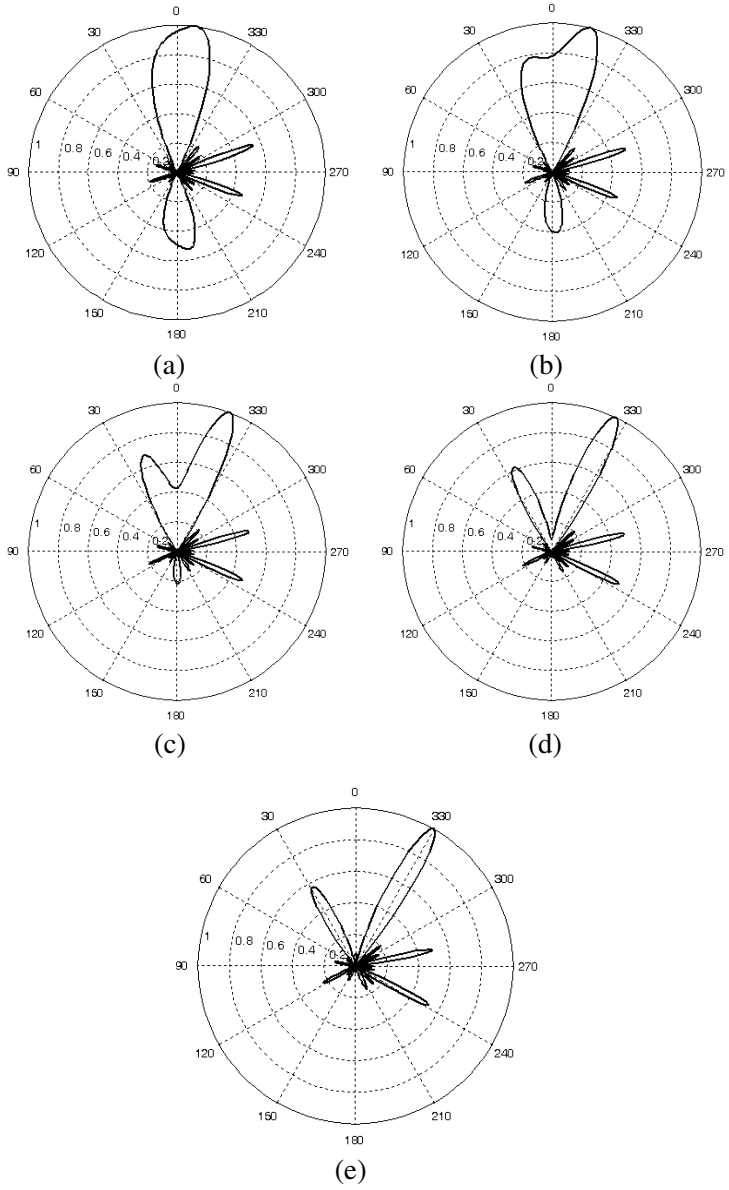

Figure 13. Radiation pattern of the $4 * 1$ phased array antenna at 28 GHz with (a) 180°, (b) 198°, (c) 216°, (d) 234°, and (e) 252° phase difference between radiating elements.

Table 2. Electrical specifications and parameters of the designed phased array antenna system.

<table>
<tr><td colspan="3">Parameter</td><td colspan="4">Value</td></tr>
<tr><td colspan="3">Array dimension and spacing</td><td colspan="4">$4 * 1$ and $3\lambda/2$</td></tr>
<tr><td rowspan="2">Return loss</td><td colspan="2">Single Antenna</td><td colspan="4">Less than -14 dB</td></tr>
<tr><td colspan="2">Array</td><td colspan="4">Less than -40 dB</td></tr>
<tr><td colspan="3">Operating frequency</td><td colspan="4">28 GHz and more</td></tr>
<tr><td rowspan="4">Cross Polarization</td><td rowspan="2">Single Antenna</td><td>E</td><td colspan="4">-13.9 dB</td></tr>
<tr><td>H</td><td colspan="4">-33.9 dB</td></tr>
<tr><td rowspan="2">Array</td><td>E</td><td colspan="4">-34.1 dB</td></tr>
<tr><td>H</td><td colspan="4">-14.9 dB</td></tr>
<tr><td rowspan="4">HPBW [Degree]</td><td rowspan="2">$\alpha = 180$</td><td>E</td><td>30.4</td><td rowspan="4">Gain [dB]</td><td rowspan="2">28</td></tr>
<tr><td>H</td><td>32.2</td></tr>
<tr><td rowspan="2">$\alpha = 252$</td><td>E</td><td>11.46</td><td rowspan="2">45</td></tr>
<tr><td>H</td><td>11.45</td></tr>
<tr><td colspan="3">SLL in the E-Plane</td><td colspan="4">-5.5 dB</td></tr>
</table>

A summary review of the designed and fabricated phased array antenna is presented in Table 2. According to this table, a perfect impedance matching has been done and a reasonable gain is achieved. Also the fractal geometry made the antenna array design to have very small and negligible cross polarized components.

3. FABRICATION PROCESS

The proposed 3-bit phased array antenna of this paper has been fabricated over N-type silicon with 100, 110, and 111 crystal network and 500 µm height. The major steps of the fabrication process were demonstrated in Figure 14. The first step is to oxidate the silicon wafer to produce a 1 µm overall layer of SiO2. Effect of this SiO2 layer on the scattering matrix parameters of the MEMS switch in ON state has been investigated in Figure 15. The simulation is done for a rectangular beam with 40 µm width.

During the sputtering process, this oxide layer would increase the adherence between CPW conductors and the silicon substrate. On the other hand, this oxide layer suppresses the wave current from passing to the substrate, which improves the insertion loss of the RF MEMS switch. Beside all these benefits, unfortunately this extra layer creates a capacitor in the gap area (G) of the CPW and affects the S_{11}

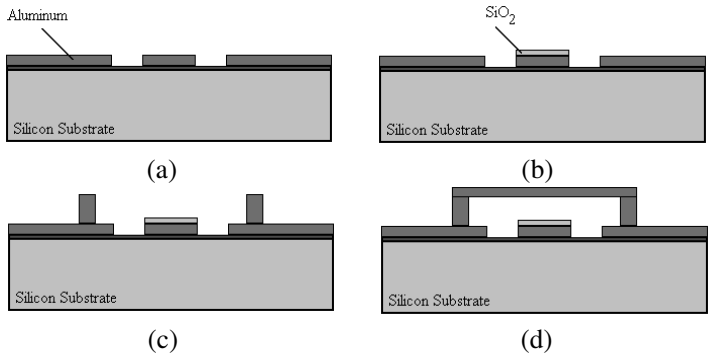

Figure 14. Fabrication process of a fractal MEMS switch using four different masks.

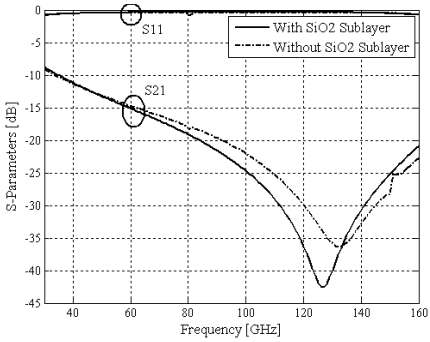

Figure 15. Effect of the 1 μm SiO2 sub-layer on the insertion and return loss of a single MEMS switch.

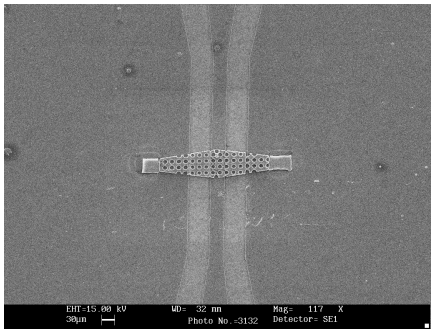

Figure 16. The fabricated capacitive switch element

parameter. So it is better to etch this extra SiO2 layer from the gap area.

Other remaining steps are quiet familiar to the designers and MEMS operators. It is majorly like, aluminium and silicon nitride layering by means of E-Beam instrument, patterning the first (CPW) and the second mask (SiN layer), layering Silicon and patterning the third mask (stones) using RIE instrument, aluminium layering and patterning the fourth mask (switch beam), and finally RIE etching of the silicon layer and making the bridge to stand straight upon the air.

The described capacitive phase shifter is fabricated and the scanning electron microscopy picture of which is presented in Figure 16.

The 5–10 μm holes over the membrane are introduced as a part of fabrication process. The RIE etching method penetrates beneath the membrane through these holes and makes it standing cross the coplanar waveguide.

4. CONCLUSION

A 3-bit and $4 * 1$ phased array antenna system has been designed using the MEMS technology. This MEMS system includes the fractal antenna elements and fractal phase shifter blocks which all have been mounted over the coplanar waveguide transmission line. It was shown that the fractal geometry made the antenna elements to have a wide frequency bandwidth, low profile, negligible cross polarized radiation, and low mutual coupling effects. Koch fractal geometry has also made the phase shifter to have very lower actuation voltage. Radiation pattern of the fabricated phased array antenna system was presented and the whole fabrication process was described in details.

REFERENCES

1. Schoebel, J., T. Buck, M. Reimann, M. Ulm, M. Schneider, A. Jourdain, G. J. Carchon, and H. A. C. Tilmans, "Design considerations and technology assessment of phased-array antenna systems with RF MEMS for automotive radar applications," *IEEE Transactions on Microwave Theory and Techniques*, Vol. 53, No. 6, Jun. 2005.
2. Gautier, W., A. Stehle, C. Siegel, B. Schoenlinner, V. Ziegler, U. Prechtel, and W. Menzel, "Hybrid integrated RF-MEMS phased array antenna at 10 GHz," *38th European Microwave Conference, EuMC 2008*, 139–142, 2008.
3. Laskar, J., S. Pinel, S. Sarkar, P. Sen, B. Perunama, M. Leung, D. Dawn, D. Yeh, F. Barale, K. Chuang, G. Iyer, J. H. Lee, and P. Melet, "60 GHz CMOS/PCB co-design and phased array technology," *IEEE Custom Integrated Circuits Conference, USA, CICC 2009*, 453–458, 2009.
4. Mousavi, P., M. Fakharzadeh, S. H. Jamali, K. Narimani, M. Hossu, H. Bolandhemmat, G. Rafi, and S. Safavi-Naeini, "A low-cost ultra low profile phased array system for mobile satellite reception using zero-knowledge beamforming algorithm," *IEEE Transactions on Antennas and Propagation*, Vol. 56, 3667–3679, Dec. 2008.
5. Van Ardenne, A., J. D. Bregman, W. A. Van Cappellen,

G. W. Kant, and J. G. B. De Vaate, "Extending the field of view with phased array techniques: Results of european SKA research," *Proceedings of the IEEE*, Vol. 97, 1531–1542, Aug. 2009.

6. Afrang, S. and B. Yeop Majlis, "Small size Ka-band distributed MEMS phase shifters using inductors," *Progress In Electromagnetics Research B*, Vol. 1, 95–113, 2008.
7. Li, L. and D. Uttamchandani, "Demonstration of a tunable RF MEMS bandpass filter using silicon foundry process," *Journal of Electromagnetic Waves and Applications*, Vol. 23, No. 2–3, 405–413, 2009.
8. Jahanbakht, M., A. A. Lotfi Neyestanak, and M. Naser Moghaddasi, "Coplanar waveguide wideband fractal koch antenna," *Microwave and Optical Technology Letters, MOP*, Vol. 50, No. 4, 936–939, Wiley, Apr. 2008.
9. Jahanbakht, M., M. N. Moghaddasi, and A. A. Lotfi Neyestanak, "Low actuation voltage ka-band fractal MEMS switch," *Progress In Electromagnetics Research C*, Vol. 5, 83–92, 2008.
10. Jahanbakht, M., M. Naser-Moghaddasi, and A. A. Lotfi Neyestanak, "Fractal beam Ku-band mems phase shifter," *Progress In Electromagnetics Research Letters*, Vol. 5, 73–85, 2008.